2D Shear Wave Elastography

LOGIQ E10, E10s, S8, LOGIQ Fortis, and LOGIQ P Series Ultrasound Systems

Introduction

Tissue stiffness is often related to underlying disease. For millennia, physicians have used palpation as a diagnostic tool to detect various ailments such as lesions, aneurysms, and inflammation. Stiff masses found during routine physical exams can be an early indication of disease, as in breast and prostate cancer. In some ailments, such as liver fibrosis, disease progression is marked by a gradual change in tissue stiffness. The ability to non-invasively measure tissue stiffness can therefore be a valuable tool in the diagnosis, staging, and management of disease.[1]

Elastography

Over the past 20 years, a number of approaches have been developed to image the mechanical properties of soft tissue non-invasively and in vivo.[2] Analogous to the process of palpation, these so-called "elastography" techniques image the tissue response to a mechanical stimulus. The tissue deformation is then used to obtain a qualitative or quantitative measure of stiffness. These methods can be classified according to the type of information portrayed, the source of excitation, and the imaging modality used to monitor tissue response, as shown in *Table 1*.

Excitation Source	Mechanical	Devices such as plates, actuators, or the imaging transducer can be applied to the skin surface to deform the underlying tissue. They can be used to apply static compression or dynamic excitation. Interstitial devices, such as intravascular balloons, can be used to induce strain in arteries.
	Acoustic Radiation Force Impulse (ARFI)	Force generated by ultrasound in tissue can be used to provide excitation to the focal region of an acoustic beam, allowing localized mechanical energy to be delivered directly to deep tissue. This force can be used to generate shear waves in tissue.
	Physiological Motion	Motion due to respiration, arterial pressure, or cardiac or other muscle activity can be used to derive elasticity information in arteries, skeletal muscle, and myocardium.
Imaging Modality	Ultrasound	The first non-invasive measurements of tissue stiffness were made with ultrasound, taking advantage of its real-time imaging capabilities and Doppler processing techniques for detecting tissue motion. Today, it remains the most widely-used imaging modality for elastography, due to fast measurement speeds (within seconds), portability, low cost, and its ability to also provide excitation with acoustic radiation force.
	MR	Often referred to as magnetic resonance elastography (MRE), this technique uses mechanical drivers to generate shear waves in the body. A 3D imaging modality, MR has the capability to measure motion with equal sensitivity in any direction. However, it is expensive, not suitable in all clinical settings, and has acquisition times on the order of minutes.
Property Displayed	Tissue Strain	Qualitative 2D image of stiffness displaying the tissue strain. High strain corresponds to a soft medium, while low strain indicates a hard medium.
	Tissue Displacement	Qualitative 2D image of stiffness displaying acoustic radiation force induced tissue displacement amplitude. High displacement corresponds to a soft medium, while low displacement indicates a hard medium.
	Shear Wave Speed or Young's Modulus	Quantitative stiffness measurement displaying the shear wave speed or Young's modulus (a measure of stiffness). Point shear wave elastography measures the average stiffness within a small region of interest (ROI) and does not show an image of stiffness. "Transient elastography" is an example of a point shear wave elastography method. 2D shear wave elastography displays an image of stiffness within an ROI.

Table 1. Summary of the major techniques used in elastography.

Shear Wave Elastography

Shear wave elastography is an imaging technique which quantifies tissue stiffness by measuring the speed of shear waves in tissue.[3] This technique uses dynamic excitation to generate shear waves in the body. The shear waves are monitored as they travel through tissue by a real-time imaging modality. Under simplifying assumptions, the shear wave speed (Ct) in a medium is related to the Young's modulus (E), which is a measure of stiffness: $E=3\rho(Ct)^2$, where ρ is density. Therefore, by estimating the shear wave speed, the underlying tissue stiffness can be quantified. A low speed corresponds to a soft medium, while a high speed indicates a stiff medium. The shear wave speed can be directly used as a proxy for stiffness or converted to Young's modulus. Shear wave elastography quantifies tissue stiffness on an absolute scale.

Shear Wave Elastography with Ultrasound

Ultrasound technology is well suited for implementing shear wave elastography. First, ultrasound can be used to generate shear waves in tissue. As sound waves propagate, a portion of their energy is transferred to the medium on the path by absorption or reflection, as shown in *Figure 1*. Application of high intensity ultrasound for a duration on the order of 100 µs generates localized displacement, which serves as a source of shear waves in tissue.[4]

GE Healthcare Curved Probe, Example

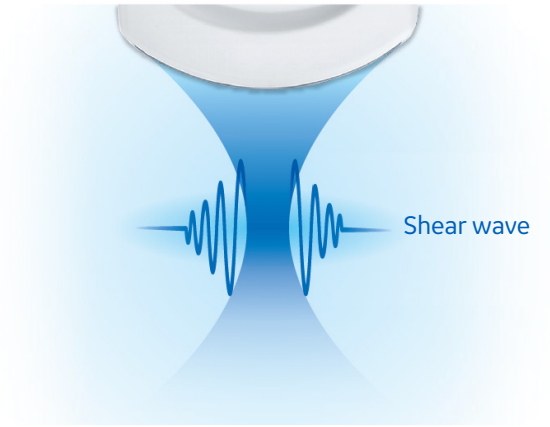

Figure 1. High intensity focused ultrasound beams can be used to push on tissue to generate shear waves, which propagate laterally away from the region of excitation.

Another advantage of ultrasound is its capability to image motion. The micron-level shear wave displacements induced by acoustic radiation force can be detected by Doppler techniques used in color flow imaging.[5]

Since the speed of sound in tissue is approximately 1,000 times faster than the shear wave speed, it is possible to use ultrasound to fully monitor the dynamics of shear wave propagation through tissue. The fact that ultrasound can provide both the stimulus to generate shear waves in tissue and the means to observe the resulting tissue response enables shear wave elastography to be performed using a single diagnostic ultrasound probe.

The **GE 2D Shear Wave Elastography suite of offerings** includes:

- LOGIQ™ E10 Series: LOGIQ E10 and LOGIQ E10s
- LOGIQ Fortis™
- LOGIQ S8
- LOGIQ P Series: LOGIQ P10, LOGIQ P9 and LOGIQ P8

2D Shear Wave Elastography Implementation

GE Healthcare has implemented shear wave elastography to display 2D images of shear wave speed or Young's modulus in an ROI. The shear wave elastography image is overlaid on the larger B-Mode image at the same location. With the B-Mode image for guidance, the user can adjust the size and position of the ROI to align to the anatomy of interest. The stiffness at any location within the ROI can be sampled to obtain a quantitative measurement of stiffness, whether in terms of shear wave speed (m/s), Young's modulus (kPa), or both. This differs from point shear wave elastography systems which measure the average stiffness within an ROI and do not display an image of stiffness. Creating an image offers several benefits. First, spatial variations in stiffness can be instantly observed. This could be useful for the detection and characterization of focal lesions. In the breast, a shear wave elastography image enables the stiffness of the hardest part of the
lesion to be quantified and compared to adjacent tissue.

Second, because shear waves induced by acoustic radiation force are small, factors such as tissue motion or poor B-Mode image quality can degrade the result. By generating a shear wave image instead of a single measurement value, the user is able to instantly perform a visual quality assessment of the result, as shown in *Figure 2*. This feedback gives the user additional information on the quality of the measurement that point shear wave elastography systems do not provide.

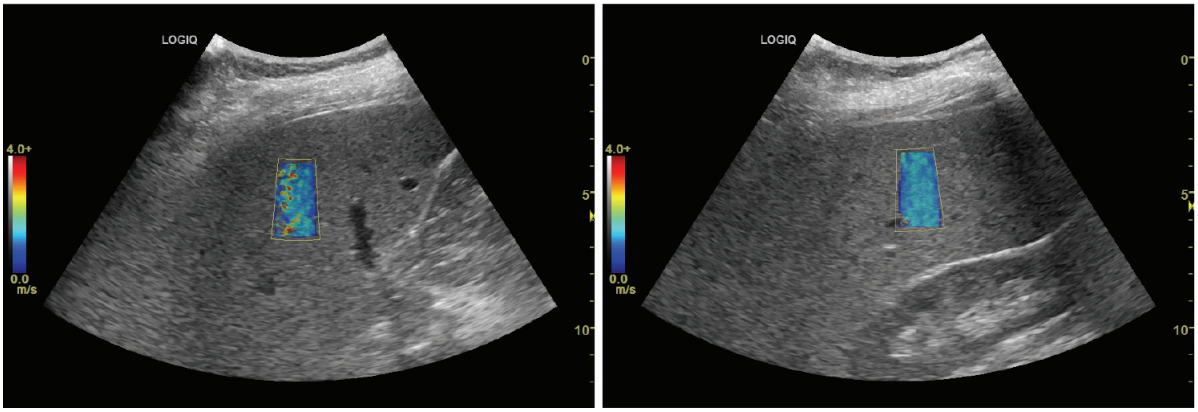

Figure 2. Examples of liver shear wave elastography images obtained on a patient with elevated liver function tests. The image on the left is degraded by artifacts on the left side of the ROI, possibly due to poor probe contact or rib shadowing. By moving the ROI to another location as shown on the right, a more homogeneous image filling the entire ROI is obtained.

2D shear wave elastography can acquire images continuously. It is important that the image displayed to the user is updated at a sufficient rate. This frame rate is dictated by two factors: the acquisition time and the cooling time. The acquisition time is how long it takes the system to acquire all the data needed to generate the image. The cooling time is the required waiting period after acquisition before the system can begin to acquire data for the next frame. Unique to shear wave elastography mode, the cooling period ensures the acoustic output of the pushing pulses meets regulatory safety levels. The acquisition time is typically on the order of 100 ms, while the cooling time is typically 1-3 seconds and is the dominant factor in limiting the frame rate. Even though the acquisition time does not significantly contribute to the frame rate, it should be minimized to reduce tissue motion artifacts. To minimize both acquisition and cooling times, 2D shear wave elastography on the LOGIQ series uses several innovative techniques.

Comb-Push Excitation

A significant challenge in using acoustic radiation force for shear wave elastography is the limited region of tissue interrogated by shear waves generated by a single focused pushing beam. One reason for the limited ROI is that the small-amplitude shear waves generated with acoustic radiation force are quickly attenuated as they propagate away from the region of excitation. In addition, shear waves are not generated at the pushing location due to inertial effects. To reconstruct the tissue stiffness over an ROI, data from multiple push locations can be combined. However, the need to transmit multiple pushes sequentially to synthesize a single 2D shear wave elastography image results in increased acquisition time. To achieve a large ROI without increasing the acquisition time, multiple pushing beams are transmitted simultaneously in a comb-like pattern, as illustrated in *Figure 3*.[6] Each pushing beam can be treated as an independent source of shear waves. As they propagate, the wave fronts generated by each push eventually meet and pass through each other. The combined wave fronts can interrogate a much larger region of tissue in a single transmit event.

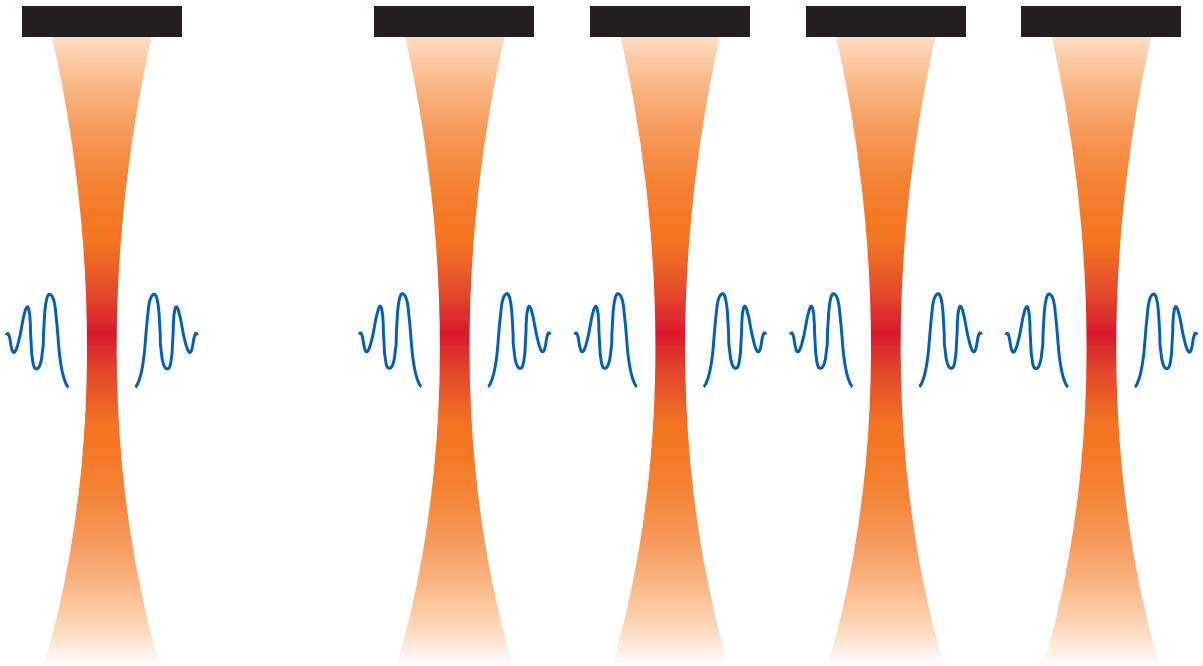

Figure 3. Comparison of single push beams and simultaneous pushing beams in a comb-like pattern. The black boxes indicate the active aperture. A single push beam is only able to generate shear wave propagation in a limited region of tissue (left). By transmitting multiple pushes in a comb-like pattern, shear waves are generated in a much larger region of tissue (right).

Time-Interleaved Shear Wave Tracking

On a conventional ultrasound scanner, the number of image lines that can be formed in parallel from a single transmit is limited. For example, a 2 cm wide ROI may be composed of 30 image lines. Shear wave motion can only be measured in a small portion of this ROI at any given time. To perform 2D shear wave elastography in a region of this size, the comb-push must be transmitted multiple times, and the tissue response tracked in a different region of the ROI each time until the entire ROI is filled. The need to retransmit the same high-intensity pushing beams multiple times requires a significant decrease in shear wave elastography frame-rate due to transducer and system heating issues as well as acoustic output concerns.

To overcome this challenge, the LOGIQ series uses a time-interleaved tracking scheme as shown in *Figure 4*. In conventional shear wave tracking, as shown in the left illustration, the comb-push is transmitted and then the tissue response is measured at all time points at a single group of image lines. The same comb-push is then retransmitted, and the motion measured at a different group. This is repeated until the tissue response in the entire ROI is measured. In the example shown in *Figure 4*, four repeated pushes are necessary. In the case of time-interleaved shear wave tracking, as shown on the right, the tissue response is sampled at a different location at every time point. This enables shear wave motion to be monitored over a wider lateral region, reducing the number of repeat pushes. In the example shown in *Figure 4*, only a single push is required to measure the tissue response in the entire ROI. This technique reduces the effective temporal sampling rate, but missing data points in time are approximately recovered by interpolation. Time-interleaved tracking enables shear wave elastography to be performed over larger ROIs without a significant reduction in frame rate.

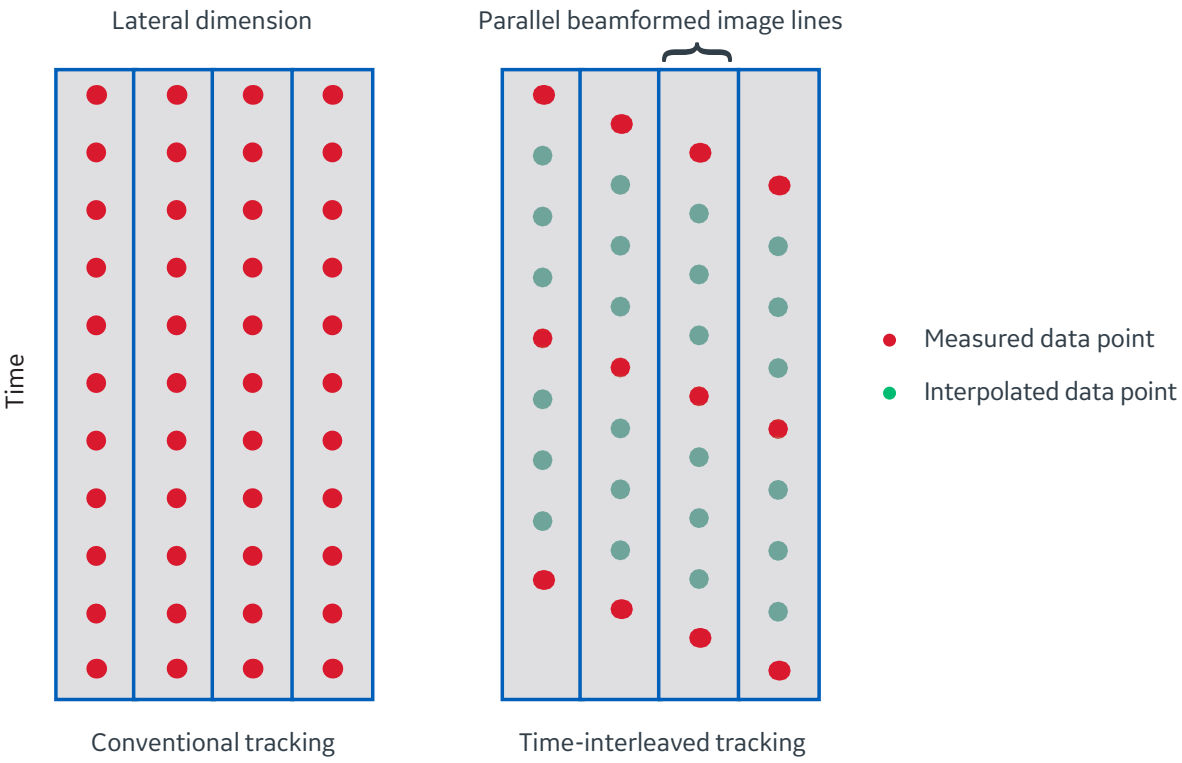

Figure 4. Conventional shear wave tracking scheme compared to time-interleaved shear wave tracking. Each column represents a group of parallel beamformed image lines within the shear wave elastography ROI.

Directional Filtering

One consequence of transmitting multiple push beams simultaneously is that a complicated shear wave field is generated, as shown in *Figure 5*. In particular, each push creates a left and right propagating wave which constructively and destructively interferes with waves generated by neighboring pushes. To make the calculation of shear wave speed easier, a directional filter is applied to separate the left and right propagating waves so they can be processed separately.[7]

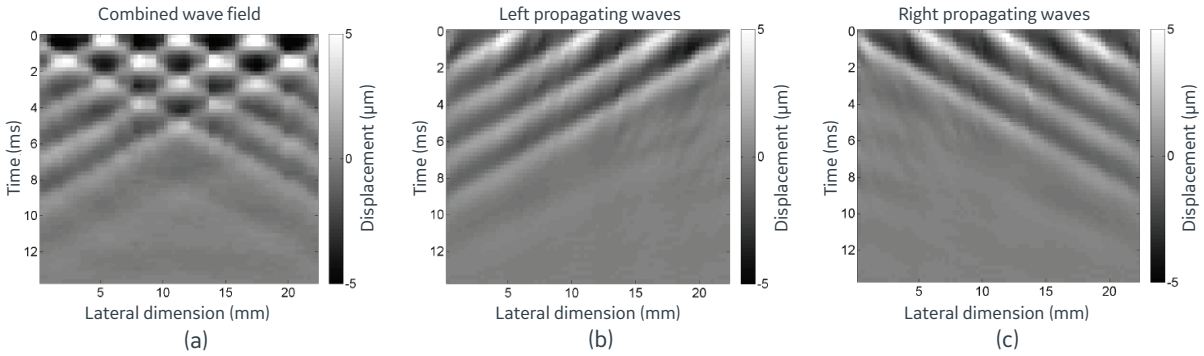

Figure 5. The shear wave displacement magnitude as a function of time and lateral location before and after directional filtering. The displacement field before directional filtering is shown in (a). There are five push beams and each one generates a left and right propagating wave which interfere with each other, complicating shear wave speed estimation. After directional filtering, this interference is removed and only waves traveling in the same direction are present, as shown in (b) for left propagating waves and (c) for right propagating waves.

Local Shear Wave Speed Estimation

A time-of-flight algorithm is used to estimate the local shear wave speed at every location in the shear wave elastography ROI. The speed at a location of interest is calculated by cross-correlating the shear wave displacement time profiles at two neighboring points, as shown in *Figure 6*. The output of the cross-correlation function gives the time taken for the shear wave to travel between the two points. By dividing the distance between the two points by the transit time, the shear wave speed is obtained. The cross-correlation function also provides the correlation coefficient, which is used to assess the quality of the measurement.

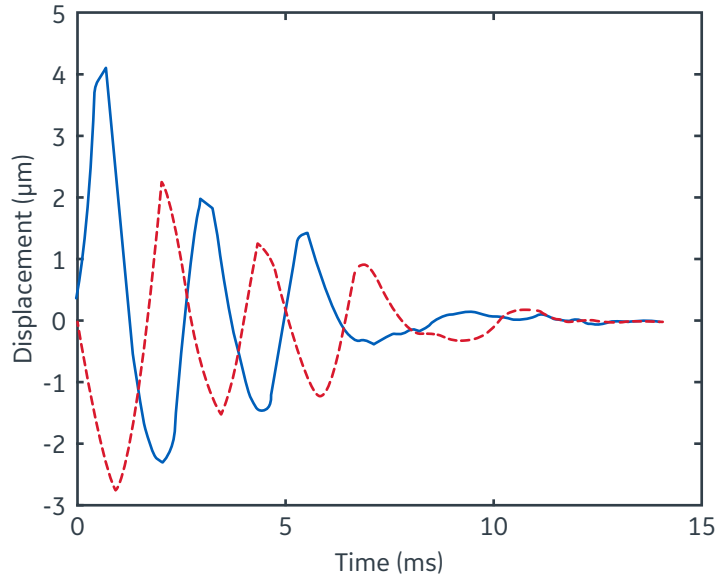

Figure 6. Shear wave displacement time profile at two locations 3.6 mm laterally apart. The time delay between the two waveforms corresponds to the time taken by the shear wave to travel between the two points. This transit time is measured by calculating the cross-correlation of the two waveforms. Dividing the distance between the two points by the transit time yields the shear wave speed between the two points, which in this case is 2.4 m/s.

This algorithm is applied independently to both the left and right propagating wave fields obtained after directional filtering, as shown in *Figure 7*. For each direction, a shear wave speed image and a correlation coefficient map are generated. The two shear wave speed images are blended using the correlation coefficient maps as weights to produce the final displayed shear wave elastography image. The correlation coefficient maps are also blended to produce a quality map which can be used to prevent areas with low measurement quality from being displayed. In the example shown in *Figure 7*, artifacts caused by blood vessels within the ROI can be removed by applying the quality threshold.

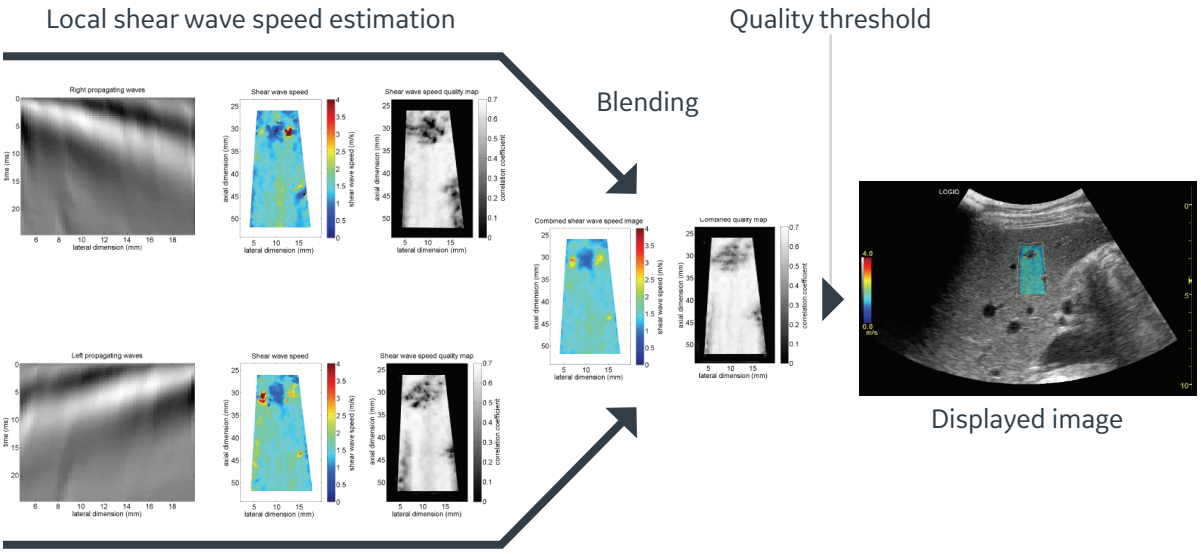

Figure 7. Shear wave speed estimation algorithm.

Clinical Application: Liver Fibrosis Staging

Liver fibrosis can result from various types of chronic damage to the liver, including infections, toxins, autoimmune disorders, and cholestatic and metabolic diseases. Cirrhosis, the end stage of fibrosis, affects millions of people worldwide. Liver fibrosis is currently staged using needle biopsy, a highly invasive procedure with a number of disadvantages.[8] These include potential morbidity and mortality, as well as susceptibility to inter-observer variability and sampling error. Additionally, repeat biopsies are not well-tolerated and therefore not suitable for monitoring disease progression.

It is well known that liver stiffness increases with the progression of fibrosis. Recently, there has been increasing interest in liver stiffness as a marker for hepatic fibrosis.

LOGIQ E10/E10s/LOGIQ Fortis

Ultrasound 2D shear wave elastography is an attractive technology for assessment of liver fibrosis as it is non-invasive, low cost, portable, and suitable for use in a variety of clinical settings. The LOGIQ E10/E10s and LOGIQ Fortis enable 2D shear wave elastography to be performed rapidly at the same time as an abdominal ultrasound exam. The LOGIQ E10/E10s and LOGIQ Fortis C1-6-D and C1-6VN-D probes are optimized for 2D liver shear wave elastography. Measurement tools are available, allowing the user to sample areas within the displayed shear wave elastography image to quantify liver stiffness. Measurements from a single exam are collected in a worksheet and summary statistics are automatically shown.

Sample Use Case

A 2D shear wave elastography evaluation of patients with biopsy-proven chronic liver disease was conducted using a post-market scanner with shear wave hardware and software equivalent to LOGIQ E10/E10s and LOGIQ Fortis. Eighteen healthy volunteers with no previous history of liver disease were also examined with 2D shear wave elastography. The subject demographics and disease etiology are summarized in *Table 2*.

Characteristic	Value
Subjects	85
Age	52 ± 16 (mean ± SD)
Sex	
Male	40 (47%)
Female	45 (53%)
Disease	
Healthy	18 (21%)
HBV	5 (6%)
HCV	43 (50%)
AIH	3 (4%)
NASH	5 (6%)
ALCOH	4 (5%)
CRYPTO	4 (5%)
PBC	1 (1%)
NDD	2 (2%)

Table 2. Subjects and demographics.
HBV = Hepatitis B virus, HCV = Hepatitis C virus, AIH = autoimmune hepatitis, NASH = nonalcoholic steatohepatitis, ALCOH = alcoholic steatohepatitis, CRYPTO = cryptogenic cirrhosis, PBC = primary biliary cirrhosis, NDD = newly diagnosed diabetes.

Data Acquisition

2D Shear wave elastography data in the liver was acquired using a GE Healthcare C1-6-D probe. Imaging was performed by two operators, each of whom had prior training and experience in HCV, acquiring shear wave elastography data using a GE Healthcare scanner on patients. During the exam, subjects were asked to lie supine with their right arm over their head. The right lobe of the liver was scanned intercostally. The shear wave elastography ROI was placed at least 1 cm below the liver capsule in a region free of vessels (if possible). Once a suitable imaging window was found, the subject was asked to suspend breathing and shear wave acquisition was initiated. After approximately five seconds, during which 2-3 shear wave image frames were typically acquired, the patient was instructed to resume breathing. If a patient had difficulty holding their breath, one shear wave image frame was obtained. This acquisition process was repeated until at least ten shear wave image frames were acquired.

After the exam, measurements were performed by placing ten circular measurement regions over the saved shear wave elastography images. The measurement regions were chosen by the operators to exclude obvious artifacts in the shear wave elastography image. Each measurement region was approximately 1 cm in diameter. The average stiffness expressed in terms of Young's modulus[9] within each measurement region was automatically recorded by the system in a worksheet. The ten measurement regions were typically placed on different shear wave image frames or at non-overlapping locations on the same frame so that ten independent measurements of liver stiffness were obtained for each subject.

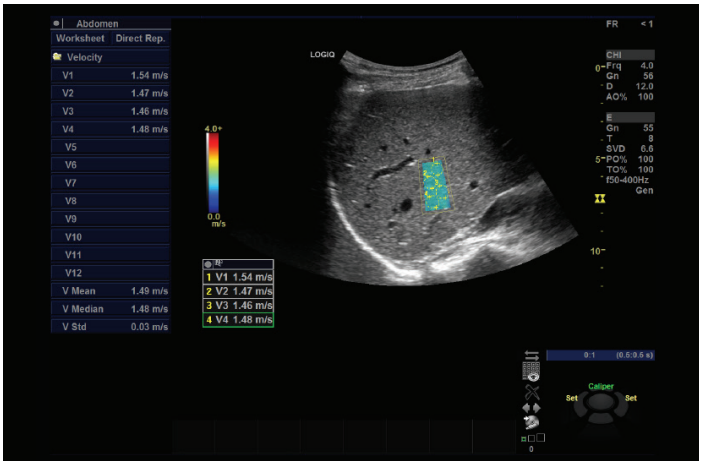

Image 1. The stiffness within multiple regions in a single shear wave image can be sampled using the measurement tool. All measurements collected in a single liver exam are listed on the left side of the display, as well as summary statistics.

Parameter	Value	m1	m2	m3	m4	m5	m6
B Mode Measurements							
E1	0.70 kPa	0.70					
E2	0.91 kPa	0.91					
E3	0.74 kPa	0.74					
E4	0.66 kPa	0.66					
E5	0.56 kPa	0.56					
E6	0.64 kPa	0.64					
E7	0.60 kPa	0.60					
E8	0.60 kPa	0.60					
E9	0.63 kPa	0.63					
E10	0.73 kPa	0.73					
E Mean	0.68 kPa	0.68					
E Median	0.65 kPa	0.65					
E Std	0.10 kPa	0.10					

Image 2. Stiffness measurements recalled from the worksheet. The user can select measurements for deletion or exclusion from calculation of the mean, median, and standard deviation.

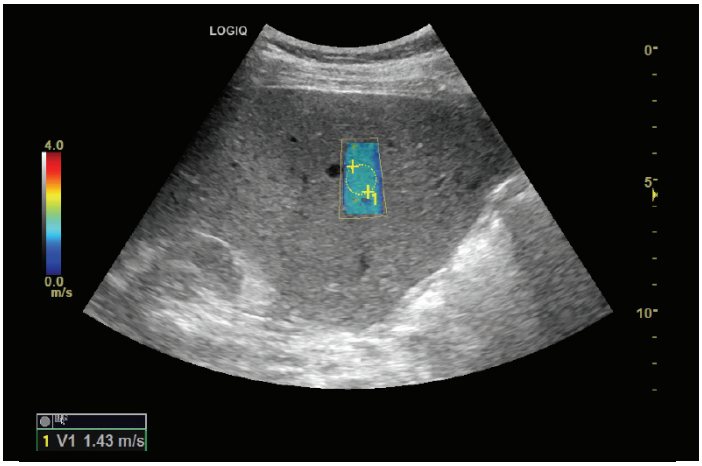

Image 3. Low liver shear wave speed measured in a patient with hepatitis C and hepatocellular carcinoma after liver transplant.

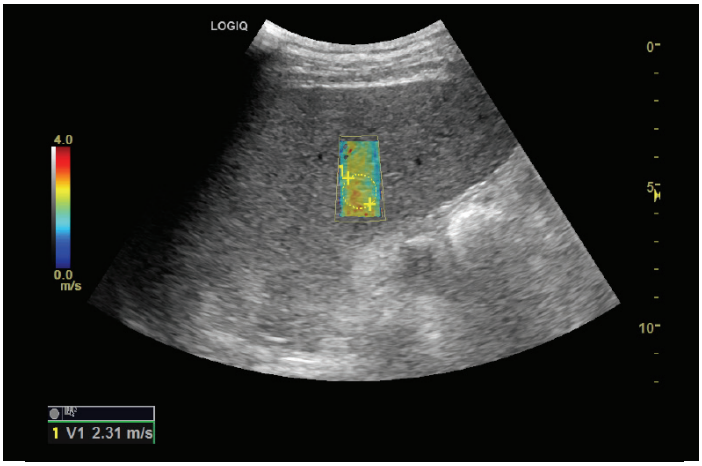

Image 4. High liver shear wave speed measured in a patient with Child-Pugh A cirrhosis.

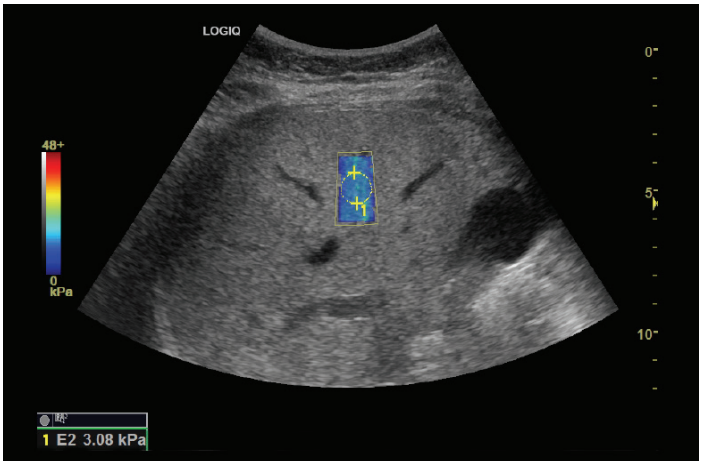

Image 5. Low liver Young's Modulus measured in a patient with stage F1 fibrosis.

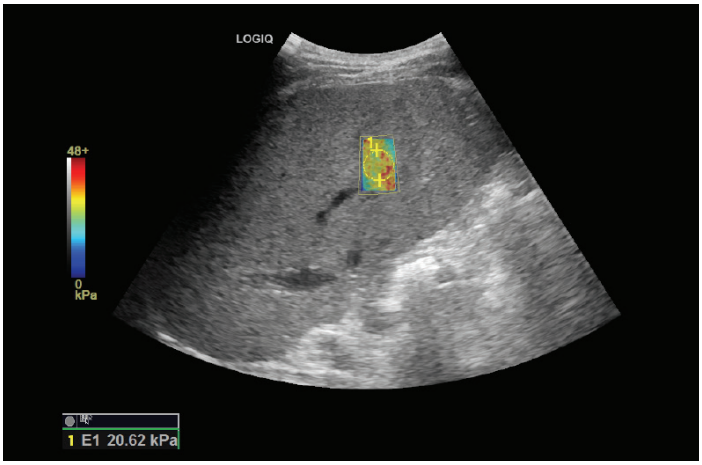

Image 6. High liver Young's Modulus measured in a patient with cirrhosis and suffering from portal hypertension and hepatitis C.

Results

The median liver stiffness from ten measurements for all subjects is shown in *Figure 8* as a function of their biopsy-proven fibrosis stage (METAVIR scale).[10] As expected, liver stiffness measured by 2D shear wave elastography increased with fibrosis. There was a correlation between liver stiffness and fibrosis stage (R2 = 0.68, p<0.001). The shear wave elastography measurements performed on each patient were reproducible, with an average interquartile range (IQR) to median ratio of 0.15 ± 0.09.

The diagnostic accuracy of LOGIQ E10/E10s and LOGIQ Fortis to measure liver stiffness for fibrosis is shown by the receiver operating characteristic (ROC) curves in *Figure 9*. Optimum cutoff values were chosen to maximize the true positive rate and minimize the false positive rate, and are shown in *Table 3*, along with the areas under the ROC curve (AUROC).

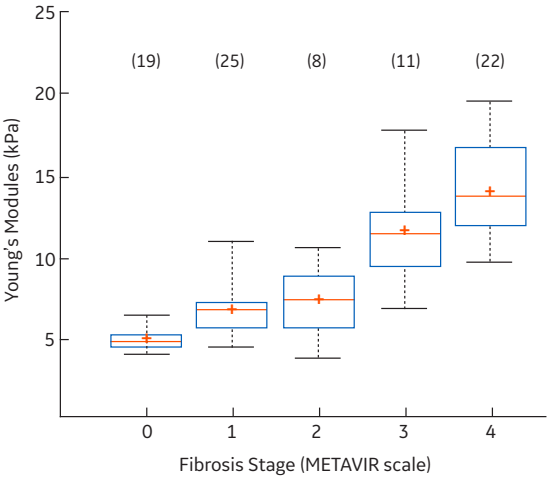

Figure 8. Median of ten liver stiffness measurements for all 85 subjects in the study, grouped by biopsy-confirmed fibrosis stage. The healthy volunteers are in the stage 0 group. The boxes represent interquartile range, while the whiskers represent the 9th and 91st percentiles.The plus sign indicates the mean, while the red line indicates the median liver stiffness of the group. The numbers in parentheses show the number of subjects in each group.

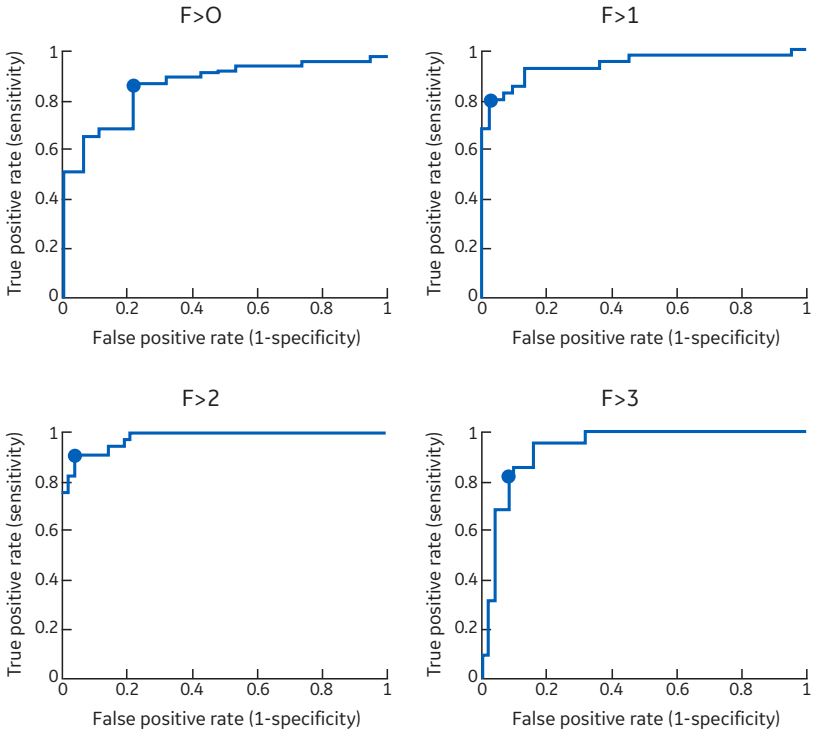

Figure 9. ROC curves for discriminating different stages of fibrosis using liver stiffness measured by the LOGIQ E9/E10/E10s/LOGIQ Fortis. The optimal cutoff which maximizes sensitivity and specificity is shown by the dots.

Liver Fibrosis Staging	Metavir Score	kPa	m/s
Absent or mild fibrosis	F1	5.48 kPa – 8.29 kPa	1.35 m/s – 1.66 m/s
Significant fibrosis	F2	8.29 kPa – 9.40 kPa	1.66 m/s – 1.77 m/s
Severe fibrosis	F3	9.40 kPa – 11.9 kPa	1.77 m/s – 1.99 m/s
Cirrhosis	F4	> 11.9 kPa	> 1.99 m/s

Table 3. Optimal LOGIQ E10/E10s/LOGIQ Fortis shear wave elastography cutoffs in terms of shear wave speed (m/s) and Young's Modulus (kPa) for classifying fibrosis stage in the patient population of this evaluation.

Discussion

This study has demonstrated that LOGIQ E10/E10s 2D shear wave elastography is a robust technique and capable of evaluating stiffness changes in the liver associated with fibrosis. Although a limited number of subjects were evaluated at the hospital in this study, liver stiffness measurements were shown to be useful for discriminating different stages of fibrosis. It is important to note that a small number of subjects with intermediate stages of fibrosis were evaluated in this study, and that a mix of disease etiologies were present. Therefore, the values shown may not be directly applicable to other patient populations. Larger studies with controlled patient demographics and disease etiology will further enhance the clinical application of this technology.

LOGIQ S8

Another study had similar findings using the LOGIQ S8 and LOGIQ P9 2D Shear Wave Elastography with respect to evaluating stiffness changes in the liver associated with fibrosis. Like the study using the LOGIQ E10/E10s, although a limited number of subjects were evaluated at the hospital, liver stiffness measurements were shown to be useful for discriminating different stages of fibrosis.

Once again, a small number of subjects with intermediate stages of fibrosis were evaluated in this study, and that a mix of disease etiologies were present. Liver stiffness measurements were shown to be useful for discriminating different stages of fibrosis, but the values shown may not be directly applicable to other patient populations.

Note: The 2D shear wave elastography data for this second study was acquired in the liver using a LOGIQ S8 R3.1.9 equivalent software and the C1-6-D probe. On the LOGIQ P9, 2D shear wave elastography data in the liver was acquired on the R3.0.0 software version, using the C1-5-RS probe. The LOGIQ P10, LOGIQ P9 R4.0.0 equivalent version used the C1-6-D and C1-5-RS probe. The LOGIQ P8 R4.0.0 equivalent version used the C1-5-RS probe.

Quality Assessment

One of the challenges of 2D shear wave measurement is that there are various inhibiting factors such as poor probe contact, probe motion, breathing, heart beating, acoustic attenuation, reflection, scattering, and rib shadowing. Quality assessment notifies these factors (artifacts) and increases clinical reliability. Quality assessment uses the cross-correlation function which is also used to estimate the local shear wave speed at every location in the shear wave elastography ROI. Thus, both shear wave speed maps and quality maps are created. This quality map can be applied by the user to prevent areas with low measurement quality from being displayed as shown in *Figure 10*.

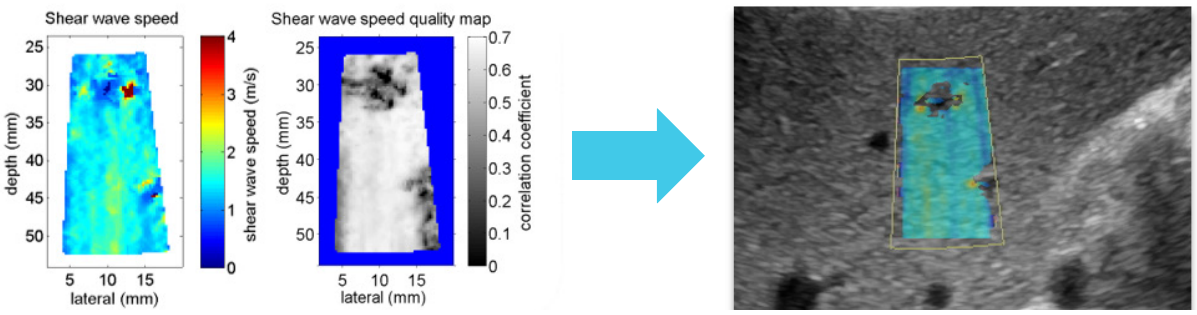

Figure 10. Quality assessment helps the user to instantly perform a visual quality assessment of the result. This feedback gives the user additional information on the quality of the measurement. In the example, artifacts caused by blood vessels within the ROI are removed by applying the quality threshold.

LOGIQ P Series

Evaluating the Effectiveness of LOGIQ P Series Shear Wave Elastography for Determining the Progression of Hepatic Fibrosis

Felix Bende, Ioan Sporea et. al. Department of Gastroenterology and Hepatology, "Victor Babeș" University of Medicine and Pharmacy Timișoara, Romania.

Background

Ultrasound shear wave elastography is becoming a standard technology for assessment of liver fibrosis[12,13] as it is non-invasive, low cost, portable, and suitable for use in a variety of clinical settings. The standard of care for staging liver fibrosis is Transient Elastography (TE), which is widely used for assessment of liver fibrosis.[14] TE has several meta-analysis studies to establish the validity of the assessments.[15,16,17,18]

Materials and Methods

Subjects

205 patients, including 78 healthy volunteers with no history of liver disease, were recruited. The average age of the subjects was 52 years (age range 15-85 years). The subject demographics and disease etiology are summarized in *Table 4*.

Data collection methods

2D Shear wave elastography data in the liver were acquired using GE Healthcare LOGIQ P Series ultrasound systems. The systems had the R3.0.0 software version and used C1-5-RS and 4C-RS probes. Ten measurements were performed and a median value was calculated as a final SWE result for each subject. Although SWE results were available for both shear wave speed in m/s and elasticity in kPa, we used elasticity value for analysis.

TE examinations were performed with a FibroScan® device (Echosens, Paris, France). During the examination, subjects were asked to lie in a supine position and raise their right arm above their head. The operator scanned the right lobe of the liver through the intercostal using the M probe (frequency 3.5 MHz) or the XL probe (frequency 2.5 MHz) and acquired ten liver stiffness values. The auto-calculated result was the median value of the ten liver stiffness values, expressed in kilopascal. The criterion of result validity was defined by interquartile range (IQR)/median value < 30% and success rate (SR) ≥ 60%.[18,19,20]

Characteristic	LOGIQ P9/P7* Values
Subjects	205
Age	53 ± 16 (mean ± SD)
Sex	
Male	106 (52%)
Female	99 (48%)
Disease	
Healthy	78
HBV	69
HCV	22
NAFLD	22
Other (AIH, PBC, ALCOH, etc.)	14

Table 4. Subjects and demographics. HBV = Hepatitis B virus, HCV = Hepatitis C virus, AIH = autoimmune Hepatitis, ALCOH = alcoholic steatohepatitis, PBC = primary biliary cirrhosis, NAFLD = nonalcoholic fatty liver disease.

Data analysis methods

After the data collection, shear wave measurements were performed by placing at least ten circular measurement regions over the stored images. The measurement regions were chosen by the operators to exclude obvious artifacts in the 2D shear wave elastography image. Each measurement region was approximately 1 cm in diameter.

The average stiffness expressed in terms of Young's modulus (kPa)[21] within each measurement region was automatically recorded by the system in a worksheet. These measurement regions were typically placed on different shear wave image frames so that independent measurements of liver stiffness were obtained for each subject. MedCalc Statistical Software version 18.11 (MedCalc Software bvba, Ostend, Belgium) was used to analyze data.

The diagnostic accuracy of this study to measure liver stiffness for fibrosis stages was calculated by the receiver operating characteristic (ROC) curves, and the optimal cutoff values were calculated from optimal criterion using Bayesian analysis. Median values of these measurements are grouped by TE criteria-confirmed fibrosis stage. The Tsochatzis meta-analysis was used to determine the stage of liver fibrosis based on the TE result, F≥2: 7 kPa; F≥3: 9.5 kPa; F=4: 12 kPa.[15, 18]

Results

The shear wave elastography stiffness value for each fibrosis stage determined by corresponding TE value according to the above criteria is shown in *Figure 11*.

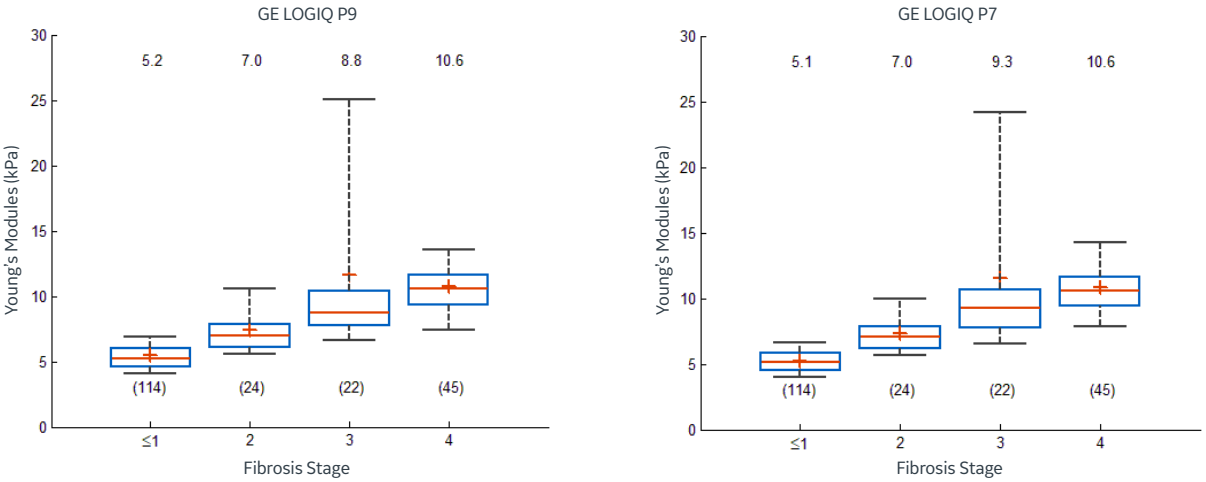

Figure 11. Median of 10 shear wave elastography measurements for 205 subjects in the study, grouped by fibrosis stage based on TE. The boxes represent interquartile range, while the whiskers represent the 9th and 91st percentiles. The plus sign indicates the mean, while the red line indicates the median value of the group. The numerical value at the top of the box-whisker shows the median value at each stage. The numbers in parentheses show the number of subjects in each group.

As expected, liver stiffness measured by LOGIQ P Series shear wave elastography increased with the level of fibrosis. There was a correlation between liver stiffness and fibrosis stage (R2 = 0.55, p < 0.001 for LOGIQ P9, R2 = 0.62, p < 0.001 for LOGIQ P7*). The ROC curves for LOGIQ P9/7 is shown in *Figures 12* and *13* and optimum cutoff values were calculated to F≥2: 6.82 kPa; F≥3: 7.60 kPa; F=4: 9.30 kPa for LOGIQ P9 and F≥2: 6.65 kPa; F≥3: 7.50 kPa; F=4: 9.30 kPa for LOGIQ P7.

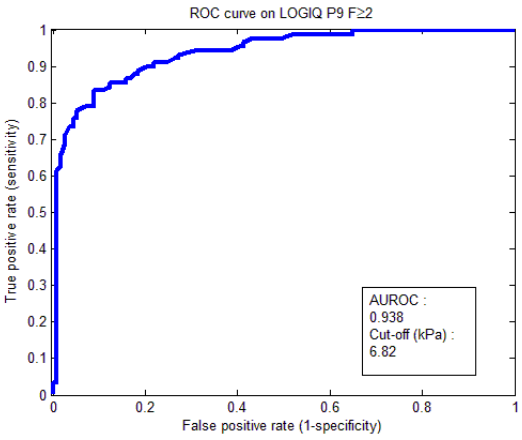

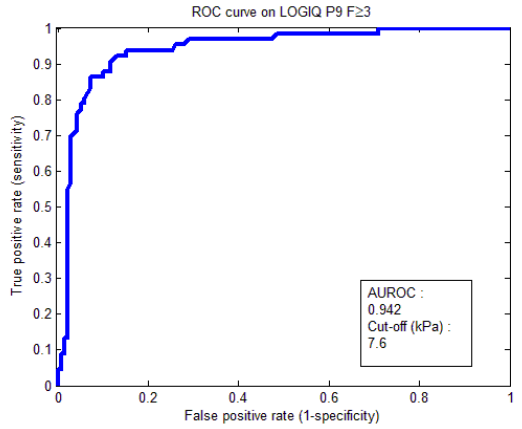

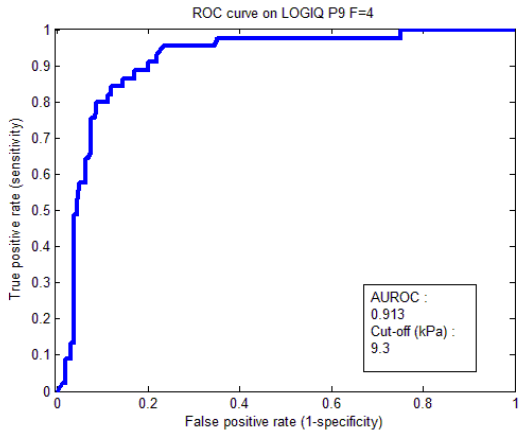

Figure 12. ROC curves for discriminating different stages of fibrosis using shear wave elastography measured by the LOGIQ P9 (C1-5-RS). The optimal cutoff values were calculated based on optimal criterion. ROC in the differentiation of stage F2 fibrosis or greater, stage F3 fibrosis or greater, and stage F4 fibrosis was 0.94 (95% confidence interval-CI: 0.90, 0.97), 0.94 (95% CI: 0.90, 0.97) and 0.91 (95% CI: 0.87, 0.95), respecitively. Cutoff values were 6.82 kPa, 7.60 kPa and 9.3 kPa with a sensitivity of 83.5%, 86.6% and 75.6%; specificity of 91.2%, 92.8%, and 92.6%, respectively.

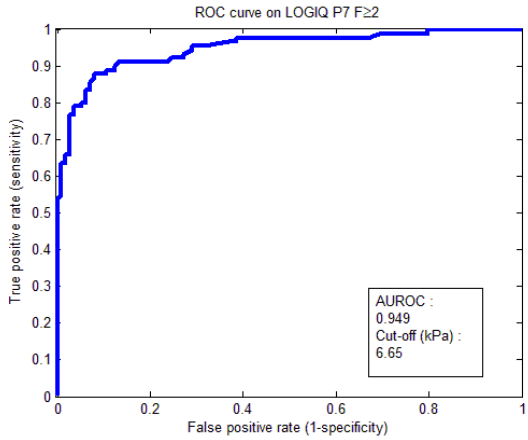

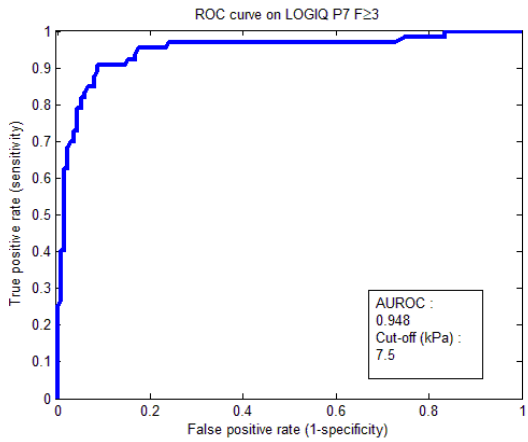

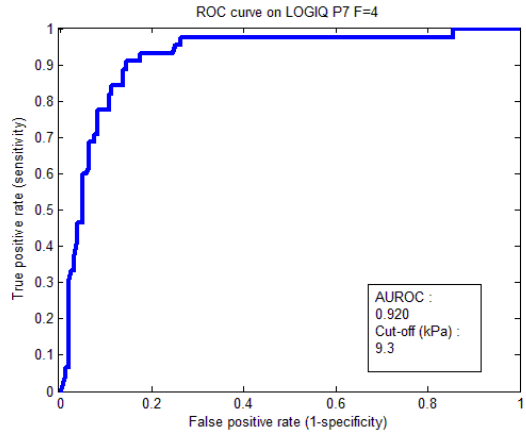

Figure 13. ROC curves for discriminating different stages of fibrosis using shear wave elastography measured by the LOGIQ P7 (4C-RS). The optimal cutoff values were calculated based on optimal criterion. ROC in the differentiation of stage F2 fibrosis or greater, stage F3 fibrosis or greater, and stage F4 fibrosis was 0.95 (95% confidence interval-CI 0.91, 0.98), 0.95 (95% CI: 0.91, 0.97) and 0.92 (95% CI: 0.87, 0.95), respectively. Cutoff values were 6.65 kPa, 7.5 kPa, and 9.3 kPa with a sensitivity of 87.9%, 91.0% and 77.8%; specificity of 92.11%, 91.3% and 91.8%, respectively.

As shown, the cutoff values for each fibrosis stage are close between LOGIQ P9 and P7. Also, two similar studies were conducted with LOGIQ S8 2D shear wave elastography, in comparison with liver biopsy (N = 90) and TE (N = 171) as a gold standard. The resulting cutoff values with liver biopsy were 6.60 kPa, 8.07 kPa, and 9.31 kPa with a sensitivity of 73.5%, 69.6%, 88.7% and 94.9%; specificity of 73.2%, 91.2%, 78.9% and 81.8%, respectively for F2, F3 and F4. The resulting cutoff values with TE were 6.9 kPa, 8.2 kPa and 9.3 kPa with a sensitivity of 85.8%, 87.5% and 85.7%; specificity of 90.2%, 86.8% and 81.2%, respectively for F2, F3 and F4.[16,17] These results are comparable to those for LOGIQ P Series in comparison with TE. Thus, a combined cutoff chart was created as shown in *Figure 14*, which can be used for the LOGIQ P Series, and LOGIQ S8.

Discussion

Fibrosis staging using Transient Elastography as the gold standard

Although a limited number of subjects and a mix of disease etiologies were evaluated in this study, liver stiffness measured by LOGIQ P Series 2D shear wave elastography increased with fibrosis, so this was shown to be useful for discriminating different stages of fibrosis.

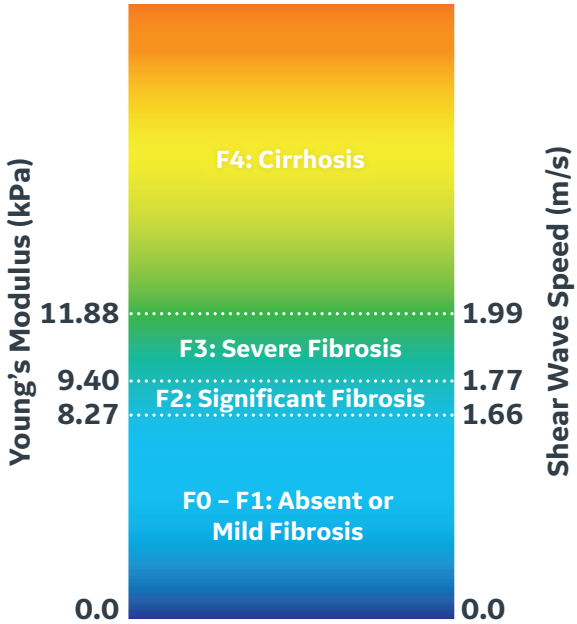

Figure 14. The combined cutoff charts. The results of LOGIQ P9/7 shear wave elastography study with TE gold standard and LOGIQ S8 shear wave elastography study with TE and liver biopsy gold standard are combined to create the chart. Left and right side express in Young's modulus value (kPa) and shear wave speed (m/s) respectively.[18]

2D Shear Wave Elastography Conclusions

The studies described in this paper show that the LOGIQ E10/E10s and LOGIQ Fortis, as well as the LOGIQ P Series, allow the user to visualize the tissue stiffness as a color-coded map in a 2D region of interest and provide the user with a quantitative measurement. Shear wave elastography is a promising technique for noninvasive quantification of tissue stiffness and has the potential to be useful in the diagnosis, staging, and management of diseases associated with changes in tissue elasticity.

Other Clinical Applications

In addition to liver fibrosis staging, there is substantial interest and research in the use of 2D shear wave elastography for other clinical applications, including breast, thyroid, prostate, and musculoskeletal (MSK) imaging. The relevant techniques for acquiring and interpreting data in these applications are still being developed.

Breast

Malignant lesions in the breast tend to be stiffer than normal breast tissue, and manual palpation is still widely used as a method for detecting breast cancer. Since 2D shear wave elastography is capable of non-invasively quantifying tissue stiffness, numerous studies have investigated its potential for classifying breast lesions. There is evidence that 2D shear wave elastography can improve the accuracy of classifying breast masses when used in addition to standard B-Mode imaging and can potentially reduce the number of biopsies.[22] In a study using a system with shear wave elastography hardware and software equivalent to the LOGIQ E10/E10s on 223 patients, 2D shear wave elastography using the 9L-D probe was able to distinguish between malignant and benign breast lesions with high sensitivity and specificity.[23] Even though these studies showed promising results, there are several significant challenges in acquiring and interpreting 2D shear wave elastography data in the breast. Compression of breast tissue with the probe can dramatically alter its stiffness and must be minimized.[24] Not all stiff lesions are malignant and not all soft lesions are benign, so shear wave elastography results must be interpreted in context of other available clinical information. In very stiff lesions, shear wave amplitude can be very low, resulting in limited propagation and poor color-fill in the shear elastography image, as well as artifacts such as a stiff rim around the edge of the lesion.[25]

Thyroid

The number of thyroid nodules (TN) identified in ultrasound exams has increased significantly in recent years due to the increased availability of high frequency ultrasound probes. However, only 5-15% of these nodules are malignant, and standard B-Mode imaging has low sensitivity in predicting malignancy. There is a clinical need for early detection and differentiation of malignant from benign TNs. Studies evaluating the potential of 2D shear wave elastography for classification of TNs have shown promising results, with malignant TNs having significantly higher stiffness than benign.[26] Factors which may confound interpretation of results include lesion size, heterogeneous lesions containing calcifications or cysts, and pathology of the nodule, with follicular carcinomas in particular tending to be soft. Besides TNs, stiffness measured by shear wave elastography has also been shown to increase in diffuse thyroid diseases such as Hashimoto's thyroiditis, Grave's disease, and Riedel thyroiditis.

Prostate

Prostate cancer (PCA) is the second highest cause of cancer deaths in men in Western countries, and its incidence has increased in recent years. Over 500,000 patients undergo prostate biopsy in the United States every year, but conventional biopsy protocol has poor detection rate for PCA and detects many insignificant PCAs that do not require treatment, resulting in overdiagnosis and treatment. Transrectal ultrasound is the most common imaging method for prostate visualization, but B-Mode has poor accuracy for diagnosing PCA, as cancerous lesions can appear isoechoic and are frequently multifocal without well-defined boundaries. Since PCA is stiffer than healthy prostate tissue, there is increasing interest in 2D shear wave elastography for the detection and localization of PCA. There is currently a limited number of studies, but all show a significantly higher stiffness for PCAs compared with benign lesions.[27] One study showed that the detection rate for PCA increased 4% when using 2D shear wave elastography for targeted biopsies.[28]

MSK

There is significant interest in quantifying the mechanical properties of muscles and tendons, as they can change with disease, exercise, injury, and rehabilitation. 2D shear wave elastography is an attractive modality for MSK as it can provide real-time visualization of stiffness changes during movement and contraction of muscles and tendons. Potential clinical applications include tendinopathy, myopathy, and sports medicine. Several studies have shown that stiffness measured by 2D shear wave elastography is higher in healthy tendons and muscles than in ones with degeneration or injury.[29,30] In addition, stiffness has been shown to change with exercise and rehabilitation of injured muscles and tendons, suggesting shear wave elastography can be used for longitudinal monitoring of the effects of healing and repair. The imaging of muscles and especially tendons is not easy, and the relevant techniques are still being developed. Both muscles and tendons are highly anisotropic, and the ultrasound beam must be oriented parallel or perpendicular to the fiber orientation for results to be meaningful. Tendon in particular is a very hard tissue, and its stiffness may exceed the maximum measurable range of the shear wave elastography system. In order to obtain reproducible results, measurement protocols must be developed to reduce the effects of voluntary contraction, fatigue and trembling, muscle contraction caused by discomfort, and orientation and position of the probe.

References

1. *Bamber, J., Cosgrove, D., Dietrich, C. F., Fromageau, J., Bojunga, J., Calliada, F., ... & Fink, M. (2013). EFSUMB guidelines and recommendations on the clinical use of ultrasound elastography. Part 1: Basic principles and technology. Ultraschall in der Medizin-European Journal of Ultrasound, 34(02), 169-184.*
2. *Greenleaf, J. F., Fatemi, M., & Insana, M. (2003). Selected methods for imaging elastic properties of biological tissues. Annual review of biomedical engineering, 5(1), 57-78.*
3. *Sarvazyan, A. P., Rudenko, O. V., Swanson, S. D., Fowlkes, J. B., & Emelianov, S. Y. (1998). Shear wave elasticity imaging: a new ultrasonic technology of medical diagnostics. Ultrasound in medicine & biology, 24(9), 1419-1435.*
4. *Nightingale, K., McAleavey, S., & Trahey, G. (2003). Shear-wave generation using acoustic radiation force: in vivo and ex vivo results. Ultrasound in medicine & biology, 29(12), 1715-1723.*
5. *Kasai, C., Namekawa, K., Koyano, A., & Omoto, R. (1985). Real-time two-dimensional blood flow imaging using an autocorrelation technique. IEEE Transactions on sonics and ultrasonics, 32(3), 458-464.*
6. *Song, P., Zhao, H., Manduca, A., Urban, M. W., Greenleaf, J. F., & Chen, S. (2012). Comb-push ultrasound shear wave elastography (CUSE): a novel method for two-dimensional shear wave elasticity imaging of soft tissues. Medical Imaging, IEEE Transactions on, 31(9), 1821-1832.*
7. *A. Manduca, D.S. Lake, S.A. Kruse, R.L. Ehman, Spatio-temporal directional filtering for improved inversion of MR elastography images, Medical Image Analysis, Volume 7, Issue 4, December 2003, Pages 465-473.*
8. *Friedman, S. L. (2003). Liver fibrosis-from bench to bedside. Journal of hepatology, 38, 38-53.*
9. *W. M. Lai, D. Rubin, and E. Krempl. Introduction to Continuum Mechanics. Elsevier, Burlington, MA, third edition, 1996.**
10. *Bedossa P, Poynard T, The METAVIR Cooperative Study Group, An algorithm for the grading of activity in chronic hepatitis C. Hepatology 1996; 24:289-93.**
11. *Song, P., Macdonald, M. C., Behler, R. H., Lanning, J. D., Wang, M. H., Urban, M. W., ... & Greenleaf, J. F. (2015). Two-dimensional shear-wave elastography on conventional ultrasound scanners with time-aligned sequential tracking (TAST) and comb-push ultrasound shear elastography (CUSE). IEEE transactions on ultrasonics, ferroelectrics, and frequency control, 62(2), 290-302.*
12. *Tada, T., Kumada, T., Toyoda, H., Ito, T., Sone, Y., Okuda, S., ... & Yasuda, E. (2015). Utility of real-time shear wave elastography for assessing liver fibrosis in patients with chronic hepatitis C infection without cirrhosis: Comparison of liver fibrosis indices. Hepatology research, 45(10), E122-E129.*
13. *Song, P., Mellema, D. C., Sheedy, S. P., Meixner, D. D., Karshen, R. M., Urban, M. W., ... & Chen, S. (2016). Performance of 2-Dimensional Ultrasound Shear Wave Elastography in Liver Fibrosis Detection Using Magnetic Resonance Elastography as the Reference Standard: A Pilot Study. Journal of Ultrasound in Medicine, 35(2), 401-412.*
14. *Bota, S., Herkner, H., Sporea, I., Salzl, P., Sirli, R., Neghina, A. M., & Peck-Radosavljevic, M. (2013). Meta-analysis: ARFI elastography versus transient elastography for the evaluation of liver fibrosis. Liver International, 33(8), 1138-1147.*
15. *Tsochatzis, E. A., Gurusamy, K. S., Ntaoula, S., Cholongitas, E., Davidson, B. R., & Burroughs, A. K. (2011). Elastography for the diagnosis of severity of fibrosis in chronic liver disease: a meta-analysis of diagnostic accuracy. Journal of hepatology, 54(4), 650-659.*
16. *Friedrich–Rust, M., Ong, M. F., Martens, S., Sarrazin, C., Bojunga, J., Zeuzem, S., & Herrmann, E. (2008). Performance of transient elastography for the staging of liver fibrosis: a meta-analysis. Gastroenterology, 134(4), 960-974.*
17. *Castéra, L., Vergniol, J., Foucher, J., Le Bail, B., Chanteloup, E., Haaser, M., ... & de Lédinghen, V. (2005). Prospective comparison of transient elastography, Fibrotest, APRI, and liver biopsy for the assessment of fibrosis in chronic hepatitis C. Gastroenterology, 128(2), 343-350.*
18. *Bende, F., Sporea, I., Sirli, R., Popescu, A., Mare, R., Miutescu, B., ... & Pienar, C. (2017). Performance of 2D-SWE. GE for predicting different stages of liver fibrosis, using Transient Elastography as the reference method. Medical ultrasonography, 19(2), 143-149.*
19. *Sandrin, L., Fourquet, B., Hasquenoph, J.M., Yon, S., Fournier, C., Mal, F., ... & Beaugrand, M. (2003). Transientelastography: a new noninvasive method for assessment of hepatic fibrosis. Ultrasound in medicine & biology, 29(12), 1705-1713.*

20. *Castéra, L., Foucher, J., Bernard, P.H., Carvalho, F., Allaix, D., Merrouche, W., ... & Lédinghen, V. (2010). Pitfalls of liver stiffness measurement: a 5-year prospective study of 13,369 examinations. Hepatology, 51(3), 828-835.*
21. *W. M. Lai, D. Rubin, and E. Krempl. Introduction to Continuum Mechanics. Elsevier, Burlington, MA, third edition, 1996.*
22. *Barr, Richard G., et al. "WFUMB guidelines and recommendations for clinical use of ultrasound elastography: Part 2: breast." Ultrasound in medicine & biology 41.5 (2015): 1148-1160.*
23. *Bayat, Mahdi, et al. "Diagnostic features of quantitative comb-push shear elastography for breast lesion differentiation." PloS one 12.3 (2017).*
24. *Barr, Richard G., and Zheng Zhang. "Effects of precompression on elasticity imaging of the breast: development of a clinically useful semiquantitative method of precompression assessment." Journal of Ultrasound in Medicine 31.6 (2012): 895-902.*
25. *Zhou, JianQiao, et al. "Breast lesions: evaluation with shear wave elastography, with special emphasis on the "stiff rim" sign." Radiology 272.1 (2014): 63-72.*
26. *Cosgrove, David, et al. "WFUMB guidelines and recommendations on the clinical use of ultrasound elastography: part 4. Thyroid." Ultrasound in medicine & biology 43.1 (2017): 4-26.*
27. *Barr, Richard G., et al. "WFUMB guidelines and recommendations on the clinical use of ultrasound elastography: Part 5. Prostate." Ultrasound in medicine & biology 43.1 (2017): 27-48.*
28. *Boehm, Katharina, et al. "Prediction of significant prostate cancer at prostate biopsy and per core detection rate of targeted and systematic biopsies using real-time shear wave elastography." Urologia internationalis 95.2 (2015): 189-196.*
29. *Ryu, Jeong Ah, and Woo Kyoung Jeong. "Current status of musculoskeletal application of shear wave elastography." Ultrasonography 36.3 (2017): 185.*
30. *Klauser, Andrea S., et al. "Sonoelastography: musculoskeletal applications." Radiology 272.3 (2014): 622-633.*

** Analysis of the data in this example was performed by GE Engineering.*

The values for the shear wave speed and tissue modulus are relative indices intended only for the purpose of comparison with other measurements performed using the LOGIQ E10, LOGIQ E10s, LOGIQ S8, LOGIQ Fortis and LOGIQ P Series. Absolute values for these measurements may vary among different measurement devices.

© 2022 General Electric Company.

GE Healthcare reserves the right to make changes in specifications and features shown herein, or discontinue the product described at any time without notice or obligation. Contact your GE Healthcare representative for the most current information. GE, the GE Monogram, LOGIQ and LOGIQ Fortis are trademarks of General Electric Company. GE Healthcare, a division of General Electric Company. GE Medical Systems, Inc., doing business as GE Healthcare.

May 2022
JB19372XX